Biosensors and Bioelectronics 164 (2020) 112332

Contents lists available at ScienceDirect

Biosensors and Bioelectronics

journal homepage: http://www.elsevier.com/locate/bios

Metal-organic frameworks-based sensitive electrochemiluminescence biosensing

Jiaojiao Zhou [a], Yun Li [a], Wenjing Wang [a], Xuecai Tan [b], Zhicheng Lu [a], Heyou Han [a,*]

[a] State Key Laboratory of Agricultural Microbiology, College of Food Science and Technology, College of Science, Huazhong Agricultural University, Wuhan, 430070, China

[b] School of Chemistry and Chemical Engineering, Guangxi University for Nationalities, Guangxi Key Laboratory of Chemistry and Engineering of Forest Products, Key Laboratory of Guangxi Colleges and Universities for Food Safety and Pharmaceutical Analytical Chemistry, Nanning 530008, China

ARTICLE INFO

Keywords:
Metal-organic frameworks
Electrochemiluminescence
Biosensor
Luminophore
Signal amplification
Modification

ABSTRACT

Metal-organic frameworks (MOFs) as porous materials have attracted much attention in various fields such as gas storage, catalysis, separation, and nanomedical engineering. However, their applications in electrochemiluminescence (ECL) biosensing are limited due to the poor conductivity, lack of modification sites, low stability and specificity, and weak biocompatibility. Integrating the functional materials into MOF structures endows MOF composites with improved conductivity and stability and facilitates the design of ECL sensors with multifunctional MOFs, which are potentially advantageous over their individual components. This review summarizes the strategies for designing ECL-active MOF composites including using luminophore as a ligand, *in situ* encapsulation of luminophore within the framework, and post-synthetic modification. As-prepared MOF composites can serve as innovative emitters, luminophore carriers, electrode modification materials and co-reaction accelerators in ECL biosensors. The sensing applications of ECl-active MOF composites in the past five years are highlighted including immunoassays, genosensors, and small molecule detection. Finally, the prospects and challenges associated with MOF composites and their related materials for ECL biosensing are tentatively proposed.

1. Introduction

Electrochemiluminescence (ECL), also defined as electrogenerated chemiluminescence, is a process in which light emitting excited states are formed through high-energy electron-transfer reactions of electrode-generated species (Miao, 2008; Richter, 2004). A Web of Science-based literature survey reveals the publication of about 7400 ECL journal articles since the first ECL study by Hercules and Bard et al. in the mid-1960s (Hercules, 1964; Santhanam and Bard, 1965). In recent years, extensive research has been performed on ECL, particularly in bioanalysis, bioimaging, nanomaterials and detection devices owing to its high sensitivity and selectivity, low background and simplified optical setup (Irkham et al., 2016; Liu et al., 2015). In 2002, Bard et al. performed the pioneering work on the ECL property of quantum dots (QDs) (Ding et al., 2002), and since then, many research efforts have been devoted to the ECL behaviors of various nanomaterials, including zero-dimensional (0D) nanomaterials, one-dimensional nanomaterials (1D), two-dimensional (2D) nanomaterials, and three-dimensional (3D) nanomaterials. Nanomaterials have been used as ECL emitters or coreaction accelerators for their versatile physical and chemical properties. For ECL emitters, QDs-based systems have been reviewed comprehensively (Zhao et al., 2015b). Coreaction accelerator could interact with the coreactant to produce more reactive intermediates and promote the reaction rate between luminophore and co-reactant, thereby producing an amplified ECL signal.

Metal-organic frameworks (MOFs) are emerging porous and crystalline materials built from metal ions/clusters and organic linkers, and have excited intense interest during the past decades (Osman et al., 2019; Wu and Yang, 2017). The brilliant features of MOFs, such as large surface area, tailorable structure and high porosity, tunable size and versatile functionality, make them promising candidates in bioanalysis and biomedical research (Gülbağça et al., 2019; Wang, 2017; Liao et al., 2019; Raza et al., 2019; Stassen et al., 2017). Despite successful development of MOFs in ECL applications, there is no comprehensive review of this topic, leading to the poor understanding of different applications of MOFs. One of the primary restraints is their low water stability, which

* Corresponding author.
E-mail address: hyhan@mail.hzau.edu.cn (H. Han).

https://doi.org/10.1016/j.bios.2020.112332
Received 6 March 2020; Received in revised form 23 May 2020; Accepted 25 May 2020
Available online 29 May 2020

tends to cause the breakdown of the framework when exposed to moisture (Aguilera-Sigalat and Bradshaw, 2016; Ge et al., 2013). Additionally, most MOFs have poor conductivity intrinsically. These defects can be overcome *via* MOF composites by integrating a variety of functional materials into MOFs or by loading guests (luminol, quantum dots, ruthenium, etc.) into MOFs (Hu et al., 2018; Xiong et al., 2015, 2017; Yang et al., 2018).

MOF composites bearing tunable pore sizes and high biocompatibility combine the advantages of both MOFs and various types of functional materials, thus integrating the individual attributes and overcoming the defects of single components. For example, Xiong et al. designed a "signal-on" ECL immunosensor by integrating $Ru(bpy)_3^{2+}$ into MOFs to fabricate $Ru(bpy)_3^{2+}$@UiO-66-NH_2 composites as the signal probes (Xiong et al., 2019). In addition to direct use of MOF composites as reporters, some MOFs that can accelerate ECL reactions can also enhance the ECL signal between luminophores and coreactants. For example, isoreticular MOF-3 (IRMOF-3) not only allows for immobilization of plentiful CdTe QDs, but also functions as self-accelerated ECL reporters, which was further utilized for cTnI immunoassay (Yang et al., 2018). Also, by using cobalt-based MOFs (Co-MOFs) as the scaffold of ECL luminophores and the co-reaction accelerator, a self-catalyzed ECL biosensor was designed for amyloid-β protein (Aβ) quantification (Wang et al., 2019a).

These composites have many distinct advantages. Firstly, emerging MOF composites, with diverse morphologies, compositions, sizes, and multifunctional capabilities, are the foundation of many applications (Hu et al., 2014). It is worth noting that the introduction of such functional materials has not significantly altered their intrinsic properties. Secondly, large surface areas and intrinsic permanent porosities endow MOF composites with high loading capacity. Thirdly, integrating luminophores and coreaction accelerators within MOF composites improves the luminous efficiency because of a short electron-transfer path. In short, the benefits of MOFs combining with various types of functional materials in MOF composites can integrate advantages from both and compensate for the disadvantages of their individual components, thus achieving synergistic effects and novel potentialities never attainable by individual parts.

The attractive characteristics of MOF composites favor the development of novel materials and their applications. In this review, we focus on MOF composites-based ECL biosensors (Fig. 1). Firstly, the basic strategies for synthesis of ECL-based MOF composites are summarized (Table 1). Secondly, the different functions of MOF composites in ECL applications are discussed. Thirdly, the illustrative examples of MOF composites-based ECL biosensors are presented. Finally, the challenges for future research are concluded, with an emphasis on the relationship between structures and functionalities of MOF composites, and the design of new devices for practical ECL applications. Different from a broad perspective on luminescent MOFs in previous reviews, this review highlights the ECL-active MOF composites from synthetic strategies to applications in multifunctional bioanalysis.

2. Designing ECL-active MOF composites

Electrochemiluminescent activity, the prerequisite for electrochemiluminescent applications of MOF composites, can be achieved through (i) using luminophore as a ligand, (ii) *in situ* encapsulation of guests or (iii) post-synthetic modification (Lin et al., 2015; Xiong et al., 2015; Xu et al., 2015). Moreover, the electrocatalytic attributes of MOFs in promoting electron or energy transfer can also be used for construction of ECL sensors (Huang et al., 2018).

2.1. Modification with ECL luminophores as ligands

The incorporation of intrinsic luminescent organic ligands provides an ideal way to prepare ECL-active MOFs due to their nano-scale porosity and well-defined nanostructures. Porphyrins and their derivatives have been extensively applied as typical ECL luminophores owing to their unique molecular electronics and molecular structures (Deng et al., 2015; Pu et al., 2019; Tokel et al., 1972). Particularly, MOF composites constructed from porphyrinic linkers have aroused great interest because of the special properties of porphyrins, such as catalytic, electrochemical, photochemical, and electrochemiluminescent

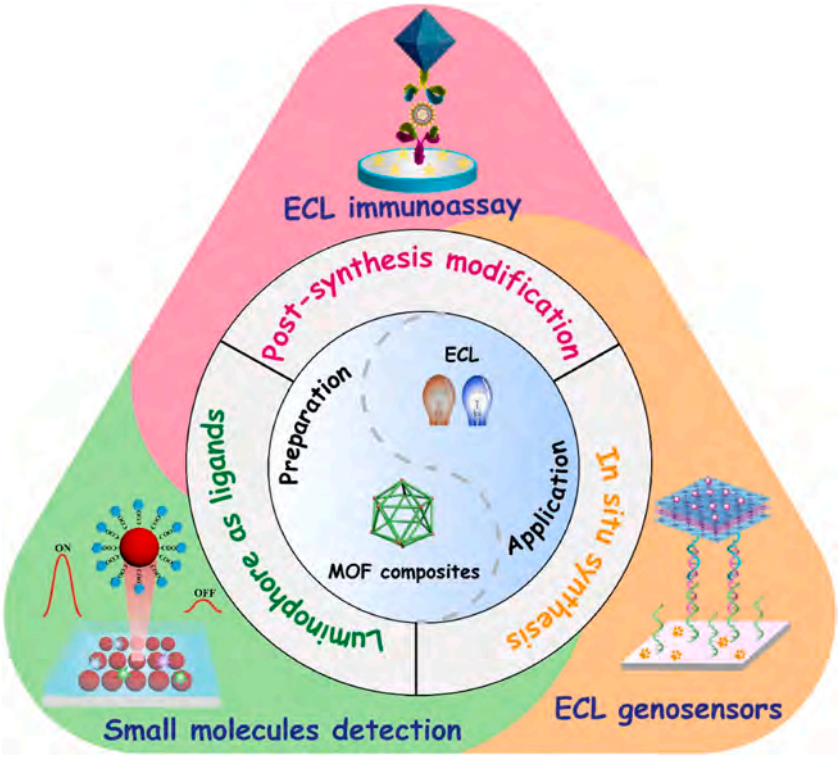

Fig. 1. Schematic illustration of preparation of MOF composites and their ECL application for biosensor development.

Table 1
Summary of various synthetic strategies of the electrochemiluminescent MOF composites.

MOF composites	Ligands	Synthesis method	Reference
Luminophores as ligands			
PCN-224	H_2TCPP	solvothermal	Wang et al. (2019c)
MOF-525-Zn	ZnTCPP	solvothermal	Zhang et al. (2016)
2D Ru-MOF nanosheets	$Ru(dcbpy)_3^{2+}$	hydrothermal	Yan et al. (2019)
Ru-MOF	$Ru(4,4'\text{-}CO_2Mebpy)_2Cl_2$	solvothermal	Xu et al. (2015)
ABEI@Fe-MIL-101	ABEI	solvothermal	Jiang et al. (2017); Wang et al. (2018b)
***In situ* synthesis**			
Ru-PEI@ZIF-8	2-methylimidazole	hydrothermal	Xiong et al. (2017)
MIL-101-CdSe	terephthalate	hydrothermal	Liu et al. (2017)
CdTe@IRMOF-3@CdTe	2-amino terephthalic acid	solvothermal	Yang et al. (2018)
Ru-MOFs	H_3btc	electrodeposition	Qin et al. (2018)
TEOA@MOFs/GO	H_3btc	solvothermal	Qin et al. (2019)
Post modification			
Fe-MIL-88 MOF	2-amino-terephthalic acid	solvothermal	Shao et al. (2018c)
Ru–PCN-777	4,4′,4′′-(1,3,5triazine-2,4,6-triyl)tribenzoic acid	solvothermal	Hu et al. (2018)
ZIF-67	2-methylimidazole	solvothermal	Wang et al. (2019e)
luminol@MIL-53(Fe)–NH_2	2-aminoterephhalic acid	solvothermal	Khoshfetrat et al. (2019)
MIL-53(Al)@CdTe-PEI	1,4-benzenedicarboxylic acid	hydrothermal	Feng et al. (2020)
MIL-53(Fe)@CdS	1,4-benzenedicarboxylic acid	solvothermal	Feng et al. (2019)

functions (Gao et al., 2014). For instance, Zhou et al. used meso-tetra (4-carboxyphenyl)porphyrin (TCPP) as a ligand for synthesis of Ce-luminescent-MOF as ECL emitters (Zhou et al., 2020b). Based on the elaborated luminescent-MOFs, they designed a "signal-off" immunosensor for sensitive quantification of proprotein convertase subtilisin/kexin type 9. Also, a three-in-one MOF-based platform was constructed from Zr-based MOFs (MOF-525-Zn) with zinc tetrakis (carboxyphenyl)-porphyrin (ZnTCPP) as the organic linkers (Fig. 2A), which was applied for accurate quantification of protein kinase A activity (Zhang et al., 2016). Additionally, porphyrins-based MOF composites could afford active sites for functional group modification. For example, porphyrin-based MOF, PCN-224 with relatively high specific surface areas and readily functionalizable sites was employed to assemble polymer dots through electrostatic adsorption to prepare the ECL probe for signal amplification (Wang et al., 2019c).

Ruthenium (Ru) is the most commonly used ECL luminophore owing to their regenerability (Carrara et al., 2017). Since the first Ru-based MOF was reported in 2010 (Kent et al., 2010), extensive studies have been conducted on the ECL behaviors of various Ru-based MOFs. Ru complexes could be integrated into MOF structures through metal ion chelation (Kozachuk et al., 2014). For instance, a redox-active MOF was designed using $Ru(dcbpy)_3^{2+}$ and Zn^{2+} by a hydrothermal method and applied in cocaine biosensing (Xu et al., 2015). In another work, as shown in Fig. 2B and D Ru-MOF nanosheets were prepared using $Ru(dcbpy)_3^{2+}$ as linkers and polyvinylpyrrolidone as structure-directing agent to form sheet-like structures (Yan et al., 2019). 2D Ru-MOF nanosheets can display more accessible active region, shorten the transportation path of ion/electron, and promote the contact with targets (Wang et al., 2017b), thus enhancing the sensing performance of MOFs. However, Ru-complexes are costly and have large steric hindrance, which restrict the load capacity to some extent and obstruct the large-scale application of $Ru(bpy)_3^{2+}$-based MOF composites. Hence it is highly desirable to develop Ru-complex-free MOFs with strong ECL intensity. Gratifying, aggregation-induced emission (AIE) luminogens display stronger ECL signal than that of the isolated one (Han et al., 2019; Peng et al., 2019). Inspired by this, AIE ligands within rigid MOFs are expected to achieve ECL enhancement. Recently, 1,1,2,2-tetra(4-carboxylbiphenyl)ethylene (H_4TCBPE), a tetraphenylethylene (TPE)-based AIEgen, was chosen as a ligand to immobilize into Hf-based MOF (Hf-TCBPE) (Fig. 2C), leading to a higher ECL intensity in comparison to H_4TCBPE aggregates and H_4TCBPE monomers (Huang et al., 2020). As mentioned above, 2D metal-organic layer (MOL) improves the utilization ratio of ECL luminophores due to the shortened diffusion paths of electrons. Xiao's group prepared a novel 2D MOL based on the AIE ligand H_4ETTC (H_4ETTC = 4′,4‴,4‴′′,4‴′′′-(ethene-1,1,2,2-tetrayl)tetrakis([1,1′-biphenyl]-4-carboxylic acid)) (Fig. 2D). The synthesized AIE luminogen (AIEgen)-based MOL yielded a stronger ECL emission because of the restriction of intramolecular motions (RIM) of the AIE ligands by coordinative immobilization (Yang et al., 2020).

Additionally, as classic ECL luminophores, luminol and its derivative-based materials have been widely applied in bioanalysis. Cui's group has successfully synthesized luminol and its derivatives modified metal nanoparticles (MNPs) by using luminophores as reducing reagents (Li et al., 2015; Shu et al., 2015; Zhang et al., 2015a). However, this modification method limited the immobilization amount due to the luminophore existed only on the surface of MNPs *via* weak covalent binding between MNPs and nitrogen atoms. To increase the loading amount, an alternative for luminophore N-(aminobutyl)-N-(ethylisoluminol) (ABEI) immobilization was developed by inserting Dox-ABEI complexes into double stranded DNA (dsDNA) (Xie et al., 2016). However, the nonconductive DNA may hinder electron transfer, thus affecting ECL signal output. To overcome these shortcomings, ABEI was used as a linker to fabricate ABEI@Fe-MIL-101 composites with excellent ECL performance because of the high load capacity of ABEI within Fe-MIL-101 (Jiang et al., 2017). Besides, the high ECL efficiency was achieved by regulating the potential to transform dissolved oxygen into superoxide radicals to accelerate the ECL reaction. Further research illustrated that ABEI@Fe-MIL-101 composites can not only be used as luminophores, but also serve as co-reaction accelerators by converting H_2O_2 into reactive oxygen radicals (Wang et al., 2018b).

2.2. *In situ encapsulation*

Encapsulation method for synthesis of MOF composites is an applicable strategy to improve their luminescence activities, including incorporation of luminescent guest molecules or nanomaterials (Lei et al., 2014). Therefore, introducing luminescent guest materials with excellent ECL efficiency into MOFs while basically maintaining the original properties of host MOFs provides an alternative approach to prepare promising ECL-active MOF composites. The *in situ* preparation of functional MOF composites takes advantage of both guest luminescent materials with desirable ECL efficiency and host MOFs with high selectivity and efficient accumulation of analytes, which may facilitate the fabrication of ECL sensing platform to precisely quantify various analytes. On the basis of large surface area of MOFs, Mo et al. combined the technique of molecular imprinting and the strong ECL emission of Fe(III)-MIL-88B–NH_2@ZnSe QDs to develop an ultrasensitive ECL biosensor for squamous cell carcinoma antigen determination (Mo et al., 2020). Fe(III)-MIL-88B–NH_2 not only enriches ZnSe QDs, but also acts as a co-reaction accelerator to substantially enhance the ECL intensity (Fig. 3A). In another work, coupled with an enzyme-assisted DNA cycle amplification method, the self-enhanced ruthenium polyethylenimine (Ru-PEI) complex enriched zeolitic imidazolate framework-8

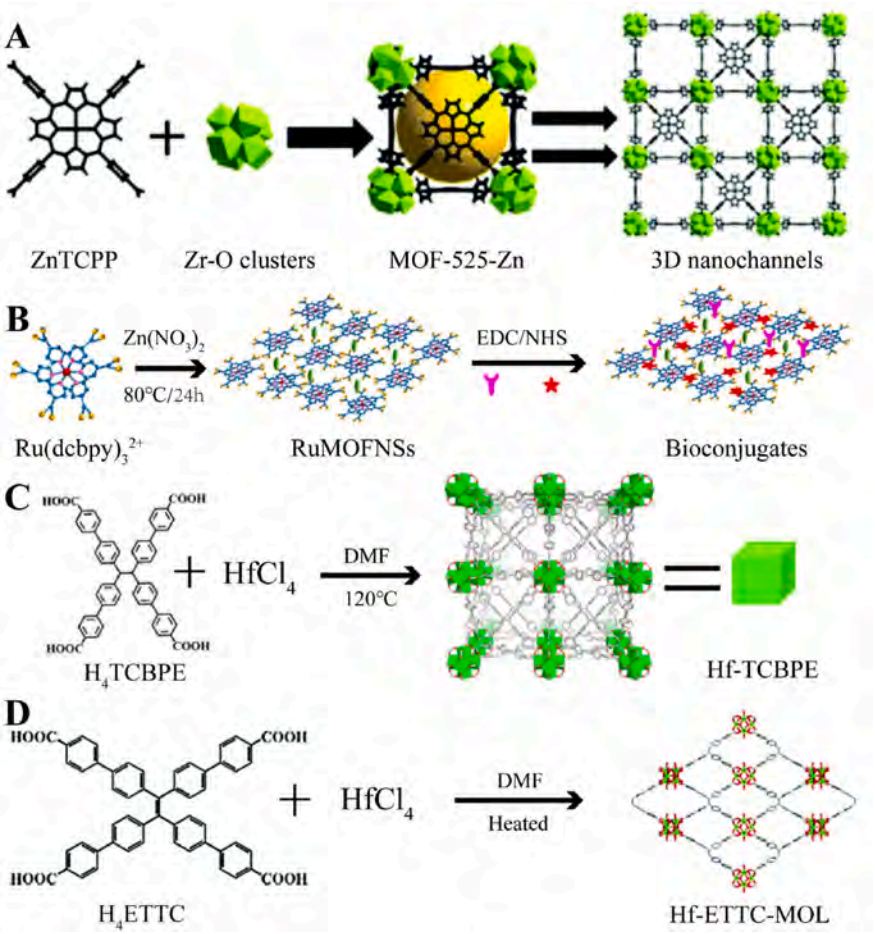

Fig. 2. (A) Illustration for the construction of zinc tetrakis (carboxyphenyl)-porphyrin MOF, MOF-525-Zn (reproduced from (Zhang et al., 2016) with permission from Royal Society of Chemistry), (B) the fabrication process of 2D MOF nanosheets (reproduced from (Yan et al., 2019) with permission from American Chemical Society), (C) synthesis of Hf-TCBPE (reproduced from (Huang et al., 2020) with permission from American Chemical Society), and (D) synthesis of the Hf-ETTC-MOL (reproduced from (Yang et al., 2020) with permission from Royal Society of Chemistry).

(Ru-PEI@ZIF-8) with superior ECL efficiency was prepared for telomerase activity detection (Xiong et al., 2017). Thanks to the porosity of ZIF-8, the ECL indicators could not only be encapsulated in the internal layer of ZIF-8, but also cover the external layer of ZIF-8, which remarkably increased the loading amount of luminophores (Fig. 3B). QDs functionalized MOFs combine the advantages of QDs with ECL activity and MOFs with efficient accumulation performance and catalyst property, leading to the enhanced ECL intensity of QDs. For example, Yang reported the enhancement of ECL efficiency by functionalizing IRMOF-3 with CdTe QDs through interior encapsulation and outer surface decoration (Yang et al., 2018). In this MOF composite, IRMOF-3 improved the ECL efficiency of QDs through promoting the transformation of $S_2O_8^{2-}$ co-reactant into sulfate radical anion ($SO_4^{\bullet-}$) (Fig. 3C).

2.3. Post-synthesis modification

As mesoporous materials, MOFs are ideal candidates to incorporate functional materials to develop novel composites with excellent ECL properties (Della Rocca et al., 2011; Huxford et al., 2010; Liu et al., 2014b). For instance, IRMOF-3 with 2-amino-terephthalic acid as a linker allows post-synthetic modification with CdTe QDs to increase the ECL intensity of CdTe (Yang et al., 2018). PCN-777 with 3.8 nm cages is an ideal vehicle to load functional materials by post-synthetic modification (Fig. 4A). Hu et al. elaborated a Ru–PCN-777 sensing platform by using PCN-777 as the carrier to support plentiful $Ru(bpy)_2(mcpbpy)^{2+}$ to increase the ECL response (Hu et al., 2018). Additionally, the strong coordination between Zr^{4+} and $-COO^-$ could effectively prevent the leakage of $Ru(bpy)_2(mcpbpy)^{2+}$. Also, MIL-53 with well-defined pore aperture, good conductivity and high surface area allows accommodation of various luminophores for ECL sensing (Feng et al., 2019; Feng et al., 2020; Khoshfetrat et al., 2019).

Designing ECL-active MOFs is an effective strategy to improve ECL efficiency and many efforts have been devoted in recent years (Xu et al., 2015; Yang et al., 2018). These composites not only boost the development of novel materials, but also broaden the application field of MOFs in ECL systems. Luminol-capped Ag nanoparticles (luminol-AgNPs) were modified on the surface of ZIF-67 through electrostatic interaction, leading to ~115-fold enhancement in ECL efficiency relative to individual luminol (Fig. 4B). Thanks to the porous structure and atomically dispersed Co^{2+}, ZIF-67 can accelerate the production of oxygen radicals (Dou et al., 2017). Furthermore, the high surface area of the ZIF-67 is favorable to load luminol-AgNPs and avoid the aggregation of AgNPs (Wang et al., 2019e).

3. MOFs in ECL biosensing

MOF composites with different chemical composition, size, shape and various interesting functions have different biosensing applications. Undoubtedly, in the ECL field, MOF composites play significant roles including new emitters, carriers, co-reaction accelerators, electrode matrices, and ECL-RET donors/acceptors. Herein, we will delineate different functions of MOFs by focusing on advanced MOF composites-based ECL systems.

3.1. MOFs as ECL emitters

Conventional ECL luminophores, such as luminol and ruthenium, have been widely used due to their low excitation potential and high ECL efficiency (Li et al., 2017a; Ma et al., 2018; Shao et al., 2014, 2016). The

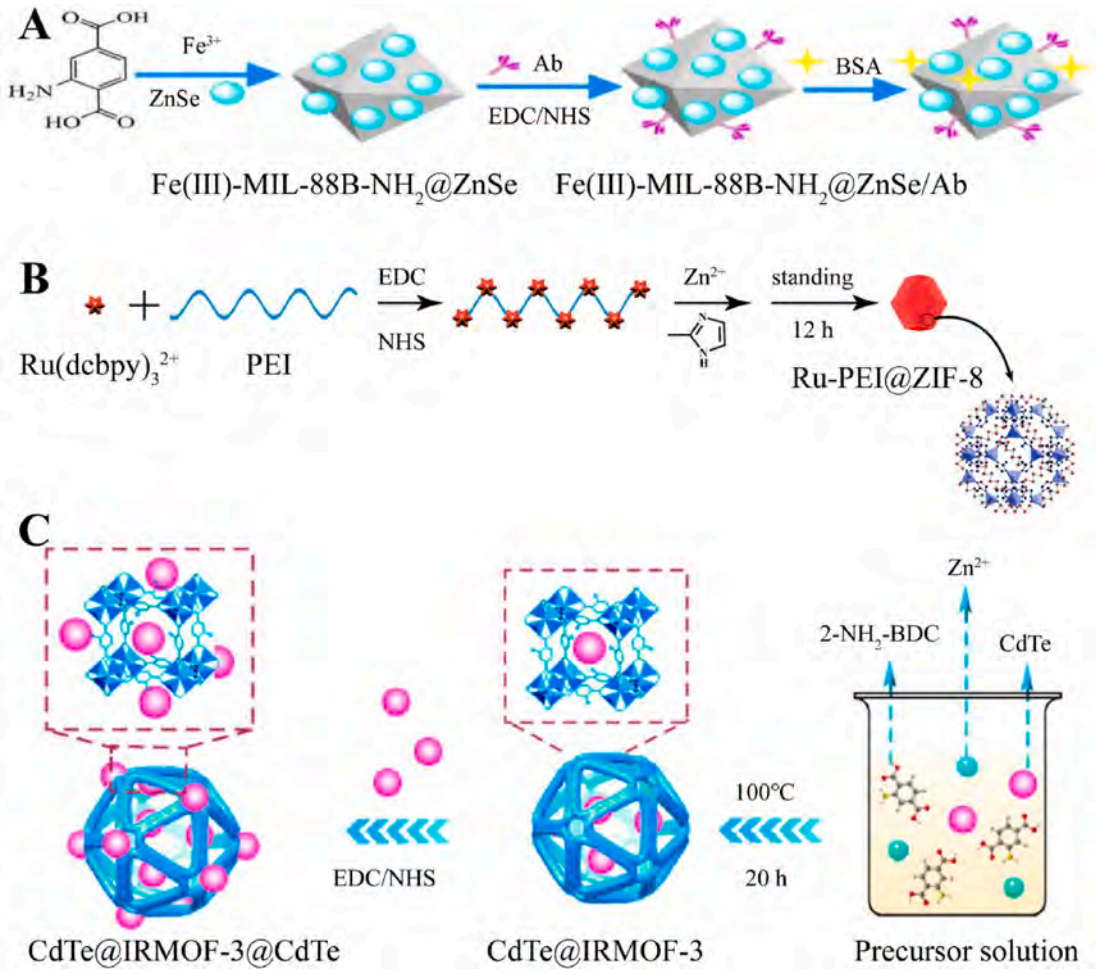

Fig. 3. (A) Preparation of Fe(III)-MIL-88B–NH_2@ZnSeQDs/Ab (reproduced from (Mo et al., 2020) with permission from Elsevier), (B) synthesis of Ru-PEI@ZIF-8 nanocomposite (reproduced from (Xiong et al., 2017) with permission from American Chemical Society), and (C) preparation of the CdTe@IRMOF-3@CdTe (reproduced from (Yang et al., 2018) with permission from American Chemical Society).

intrinsic properties of MOFs are unique benefits that make them promising candidates for storage (Miao et al., 2017; Wang et al., 2016c), catalysis (Lee et al., 2009; Wu and Zhao, 2017) and biosensing (Qi et al., 2019; Ren et al., 2018). The marriage of MOFs and ECL luminophores achieves the combination of their individual merits. Designing ECL-active MOF is crucial for ECL application. Among the synthetic methods for ECL-active MOFs, the use of luminophores as ligands is superior to other methods due to the simple synthesis process, high loading capacity of luminophores, and no leakage of luminophores inside MOFs. Thus, functionalized MOFs with luminophores as ligands would be promising emitters in ECL sensing owing to their desirable ECL properties, low toxicity and biocompatibility.

Introducing ECL luminophores as organic ligands is an approach to fabricate ECL-active MOFs as emitters (Xiong et al., 2015; Xu et al., 2015; Zhu et al., 2017). For example, Yuan's group used $[Ru(dcbpy)_3]^{2+}$ as the organic ligand to synthesize MOFs with excellent ECL performance for N-terminal pro-B-type natriuretic peptide (NT-proBNP) determination (Xiong et al., 2015). Various hierarchical nanostructures, such as MOF nanoflowers (Wang et al., 2019a; Zhu et al., 2017), 2D MOF nanosheets (Shao et al., 2018b; Yan et al., 2019), 2D MOF nanoplates (Yao et al., 2019), and porous MOF materials (Ma et al., 2016a) have been synthesized as suitable ECL emitters. The nanoflower-like functional MOFs can be used to fabricate sensors with various merits like large surface area, convenient charge transport, and low cost (Karimi and Morsali, 2013). Similarly, by exposing more accessible active sites on its surface and shortening the distance from luminophores to substrates, 2D MOF nanosheets further improve the sensing performance of MOFs (Huang et al., 2017; Zhao et al., 2015a). On the basis of the synergic self-assembly reaction of Zn^{2+} and $Ru(dcbpy)_3^{2+}$, Wang synthesized novel Ru-MOF nanosheets *via* a simple one-pot strategy, which not only increased the load capacity, but also prevented luminophore leakage (Yan et al., 2019). Yuan's group synthesized ruthenium complex doped MOF nanoplates *via* a mixed ligand strategy (Yao et al., 2019), which was relatively easy to prepare and can avoid the complicated post-synthetic steps. The system of 2D nanoplates with the merits of shortened energy and electron transfer path and enhanced ECL efficiency showed promising performance in bioanalysis. For instance, Ma et al. obtained porous cyclodextrins (CDs)-based MOFs through coordination of CDs with metal ions, which showed unexpected reducing capacity toward $AuCl_4^-$. As a result, Au NPs were *in situ* formed on Pb-β-CD without adding any other reductant, leading to the enhanced ECL intensity and increased biocompatibility of Pb-β-CD (Ma et al., 2016a). On the basis of the high ECL properties of MOF nanostructures, various ECL biosensors have been constructed for the rapid detection of metal ions, small molecules, proteins, and nucleic acids, which will be described in detail in another section.

As a typical derivative of luminol, ABEI could be functionalized more easily with MOFs than luminol due to an extra primary amine away from benzene ring (Xie et al., 2018). For instance, Jiang et al. used ABEI modified MOF (ABEI@Fe-MIL-101) as the efficient ECL reporter and designed an ECL immunosensor for the measurement of mucin1 on cancer cells (Jiang et al., 2017). To date, multifarious strategies have

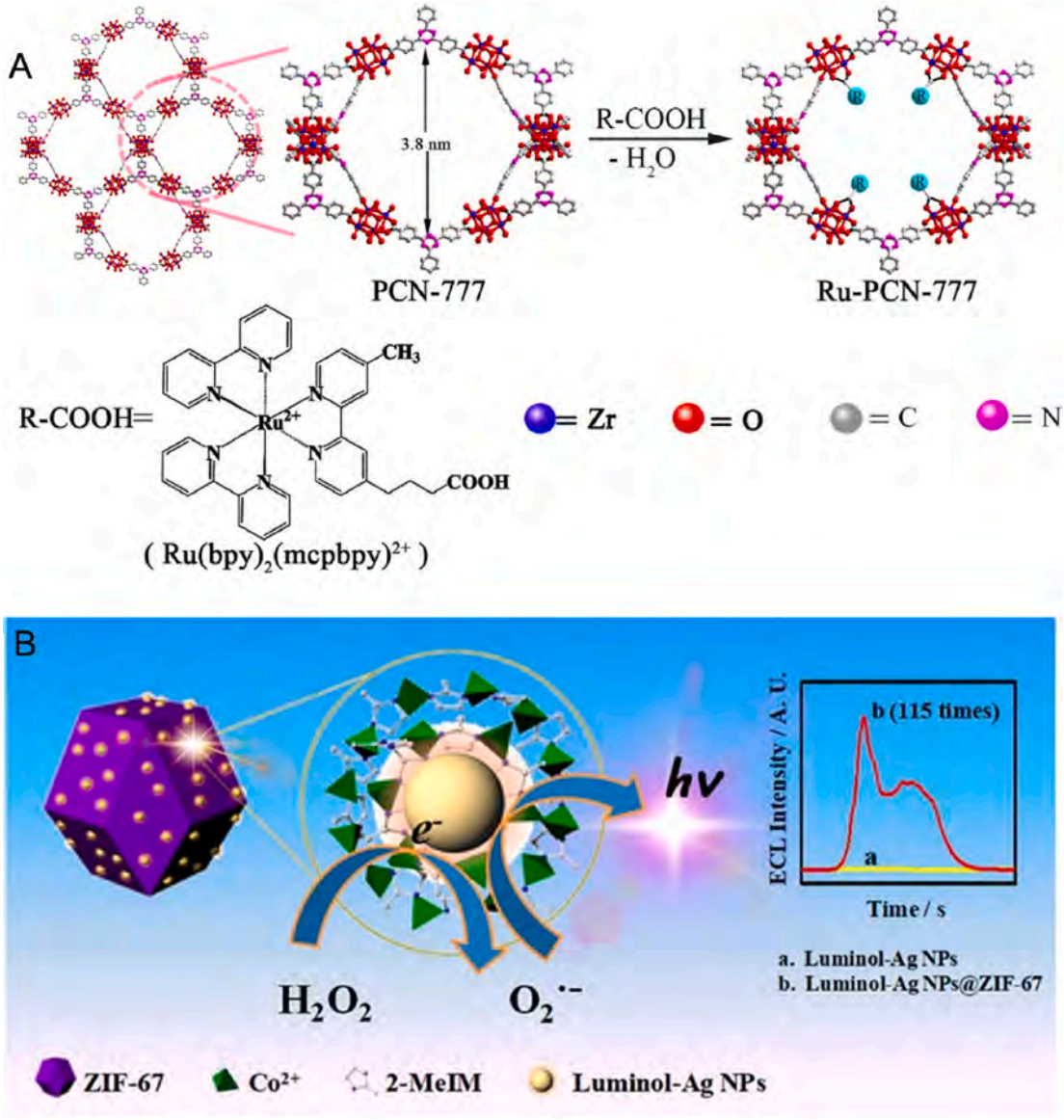

Fig. 4. (A) Schematic depiction of incorporating $Ru(bpy)_2(mcpbpy)^{2+}$ inside the channels of PCN-777 through the solvent-assisted ligand incorporation approach (reproduced from (Hu et al., 2018) with permission from American Chemical Society), and (B) schematic illustration of the integration of Co-based MOF and AgNPs for the enhancement of luminol ECL (reproduced from (Wang et al., 2019a) with permission from American Chemical Society).

been proposed to increase the ECL signal of luminol derivatives, such as utilizing nanomaterials as mimic peroxidases to catalyze coreactant H_2O_2 (Jiang et al., 2015; Wang et al., 2016b), and generating H_2O_2 *in situ* (Cao et al., 2012; Jiang et al., 2013). Due to their intriguing properties, MOFs also have great potential in catalysis. Among various MOFs, Fe(III)-based MOFs such as MIL-53 (Liu et al., 2013), MIL-88 (Chen et al., 2015), and MIL-101 (Ai et al., 2013) have been applied to catalyze H_2O_2. For example, MIL-101(Fe) serves not only as an effective vehicle to load ABEI, but also as an intrinsic mimic peroxidase for H_2O_2 decomposition (Fig. 5A). Additionally, Au NPs with high biocompatibility were modified on ABEI/MIL-101(Fe) to immobilize antibody for the sensitive MUC1 determination (Wang et al., 2018b).

3.2. MOFs as carriers

Apart from ECL emitters, the porous structures and unique catalytic properties of MOFs can also serve as carriers for ECL luminophores to amplify ECL signal. Luminol and its derivatives, $Ru(bpy)_3^{2+}$ and its derivatives, and QDs are common luminophores loaded in various MOFs. The most popular MOFs as carriers are zirconium-based MOFs (especially UiO-66/67), Zn-based MOFs and Fe(III)-based MOFs.

The cubic UiO-66 solids are excellent nanocarriers to load guest molecules owing to their two octahedral (≈11 Å) and tetrahedral (≈8 Å) cavities, non-toxicities, and desirable stabilities (Cunha et al., 2013; Vermoortele et al., 2013). Recently, Dong et al. elaborated an ultrasensitive competitive method-based diethylstilbestrol sensing platform by encapsulating $Ru(bpy)_3^{2+}$ in UiO-67 for ECL signal amplification (Dong et al., 2018). UiO-67 acts as the carriers with a large specific surface area for $Ru(bpy)_3^{2+}$ loading and antibody modification. Aside from carrying small molecules, zirconium-based MOFs have been also used for loading nanocrystals by chemical modification. Wang et al. synthesized UiO-66-NH_2 with mesoporous cages by thermally treating at 300 °C to remove a part of organic functionalities (Wang et al., 2020). The prepared UiO-66-NH_2 not only serves as the anchor carrier for the enrichment of Mn doped ZnAgInS nanocrystals, but also alleviates the inner filter effect efficaciously (Fig. 5B). Ju's group constructed a dual ECL RET biosensor for detection of two kinds of proteins on the cell surface, with PCN-224 as the vehicle to assemble the DNA functionalized

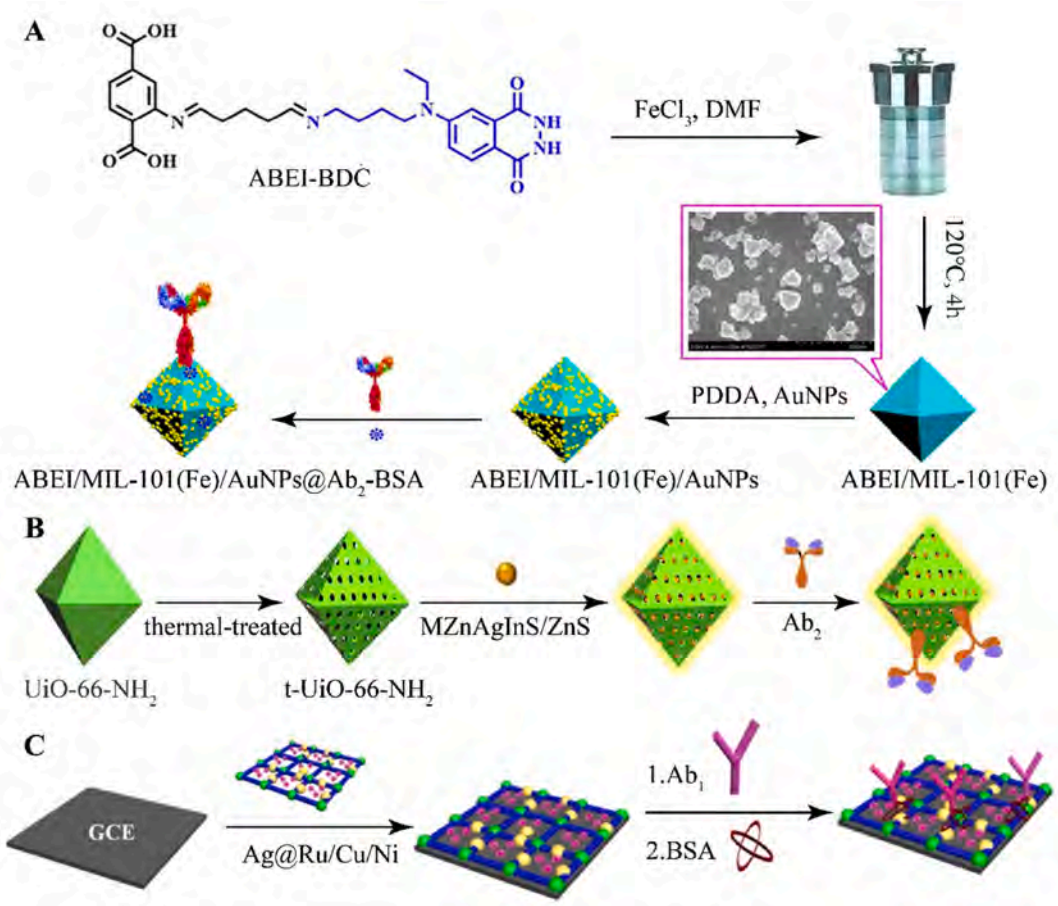

Fig. 5. (A) Synthesis of ABEI/MIL-101(Fe)-AuNPs@Ab_2-BSA bioconjugates (reproduced from (Wang et al., 2018b) with permission from Elsevier), (B) Preparation of luminophore and Ab_2 bioconjugates (reproduced from (Wang et al., 2020) with permission from Elsevier), (C) Synthesis of (Ag@Ru/Cu/Ni)@Ab2-BSA bioconjugates (reproduced from (Li et al., 2017b) with permission from Elsevier).

polymer dots for the enhancement of ECL signal (Wang et al., 2019c). Additionally, UiO-66 has also been reported to load catalysts such as Au NPs and Pt NPs to catalyze luminol/H_2O_2 ECL system (Yan et al., 2018).

Zn-based MOFs have also served as carriers because of its large enough dimensions to adsorb chromophoric building blocks. For instance, Zhao et al. designed a novel 3D $Ru(bpy)_3^{2+}$ caged zinc oxalate MOF, which shielded the chromophores from solvent and resulted in high ECL efficiency due to the rapid energy transfer among $Ru(bpy)_3^{2+}$ within the 3D network (Zhao et al., 2019). Furthermore, Au@NiFe MOFs are applied as dual quenchers to $Ru(bpy)_3^{2+}$ loaded zinc oxalate MOFs due to the ECL-RET between $Ru(bpy)_3^{2+}$/zinc oxalate MOFs (donor) and Au@NiFe MOFs (acceptor).

Fe(III)-based MOFs have become another common carriers for ECL applications due to their good water solubility, controlled size and large surface area. For example, Shao et al. prepared Fe-MIL-88 MOFs as the carriers of Au NPs and hemin to construct a target-triggered ratiometric ECL sensors to determine PSA *via* the "competition" model (Shao et al., 2018c). Recently, Feng proposed an aptasensor to detect kanamycin and neomycin using an ECL-RET approach based on MIL-53(Fe) as carriers of CdS QDs (Feng et al., 2019).

Moreover, the ECL efficiency of MOF composites can be further improved by reducing its dimension from 3D bulk to 2D layer. 2D MOF nanosheets have the intrinsic advantage over 3D MOF crystals in increasing the loading amount of luminophores, shortening the electron transfer distance and reducing the diffusional constraints of electron, leading to great enhancement in ECL efficiency and intensity. Recently, Hu et al. reported a novel Ru-grafted 2D metal-organic layer (Ru-MOL) with PEI as co-reactant to increase the ECL intensity, achieving 14.5-fold enhanced ECL efficiency relative to 3D PEI@Ru–PCN-777 composites (Hu et al., 2019). Also, Yang et al. prepared an ultrathin 2D MOL for grafting self-enhanced ruthenium complexes with 93.45-fold ECL intensity enhancement over 3D Ru-MOFs (Yang et al., 2019).

3.3. *MOFs for electrode modification*

Electrode modification is one of the most important steps for biosensing platform construction. Due to the good water solubility and poor film forming capacity of classic ECL luminophores, luminol and ruthenium on the electrode, considerable efforts have been made to improve immobilization of luminophores on electrode surfaces to enhance the ECL signal.

MOFs are not only ideal carriers to load ECL illuminants, but also promising materials for electrode modification. For instance, $Ru(bpy)_3^{2+}$ modified 3D CuNi oxalate MOFs were decorated on the electrode surface to improve the luminescence activity of MOFs for CEA detection (Li et al., 2017b). Additionally, Ag nanoparticles were used to functionalize the MOF composites (Ag@Ru/Cu/Ni) to amplify ECL signal and to facilitate antibody absorption on the modified-electrode surface (Fig. 5C). Ma et al. fabricated a label-free ECL immunosensor for detecting PSA by modifying Ag nanoparticles-doped Pb(II) MOF onto GCE surface to form a sensing platform (Ma et al., 2016b).

It is firmly believed that solid-state ECL platform is highly superior to solution-phase ECL system in terms of ECL efficiency enhancement, reagent reduction and design approach simplification (Wei and Wang, 2008). For this reason, some efforts have been taken to build solid-state ECL platforms and propose effective strategies for immobilization of Ru

$(bpy)_3^{2+}$ on electrode surfaces. For instance, Li et al. used $Ru(bpy)_3^{2+}$ caged Zn(II) MOFs as a solid ECL tag, based on which a label-free ECL sensor was proposed for dopamine measurement (Li et al., 2018). However, tripropylamine (TPA) as the most common co-reactant of $Ru(bpy)_3^{2+}$, is toxic and volatile, thus limiting its application and affecting the experimental accuracy. Since $Ru(bpy)_3^{2+}$ can react with amides, compounds with plentiful amine can serve as effective co-reactants of $Ru(bpy)_3^{2+}$ to boost ECL emission. Recently, Wu's group employed melamine (1,3,5-triazine-2,4,6-triamine) as a co-reactant to fabricate solid-state ECL sensor for melamine detection (Feng et al., 2018). In another work, a higher ECL signal was generated from the Ru-MOF modified electrode, indicating the ease of electron transfer between Ru-MOF and co-reactants. These results facilitate a better understanding of MOFs, co-reactants and electrodes and highlight the potential of MOFs in the application of ECL systems.

3.4. Multifunctional MOF composites

With the rapid development of sensors and biosensors, individual MOF cannot meet the current requirements for ultrasensitive analysis. Thus, multifunctional MOF composites with different performances have attracted increasing interests in analytical applications.

In a series of ECL immunosensors designed by Qin's group, different multifunctional MOF composites have been applied. For example, NH_2-MIL-53(Al) not only served as the supporter of palladium nanoparticles (Pd NPs), but also as an ECL acceptor in a ECL RET system. (Fang et al., 2019a). In another report, ABEI decorated Co-MOFs (Co-MOFs/ABEI) not only functioned as a carrier to load ABEI, but also acted as a co-reaction accelerator to catalyze H_2O_2 decomposition (Wang et al., 2019a). Similarly, Yuan's group developed an ABEI modified Fe-based MOF (ABEI/MIL-101(Fe) (II) with the functions of both catalyzer and luminophore (Wang et al., 2018b). In an ECL immunosensor for detecting PSA, MIL-53(Fe)–NH_2 was utilized as a carrier of luminol and a co-reaction accelerator (Khoshfetrat et al., 2019). In another report on PSA detection, Fang et al. prepared Ag^+@UiO-66-NH_2 to load CdWS luminophores, resulting in improved ECL intensity of the sensors. Besides, Ag^+@UiO-66-NH_2 was also used as a coreaction accelerator in the CdWS/$S_2O_8^{2-}$ system through the transformation of $S_2O_8^{2-}$ into $SO_4^{\bullet-}$, which amplified the ECL signal of the system (Fang et al., 2019b). Recently, Wang et al. reported an ECL aptasensor using g-C_3N_4 nanosheets and $Ru(bpy)_3^{2+}$ doped MOFs as energy donor-receptor pairs. It is worth noting that MOFs were used as both a luminophore carrier and a coreaction accelerator to enhance the ECL intensity of the system (Wang et al., 2019f).

3.5. MOF composites as ECL-RET donors or acceptors

ECL-RET has been proposed as an efficient sensing approach recently (Cao et al., 2019; Chen et al., 2018; Liu et al., 2018; Xue et al., 2019b), which may occur when the donors' emission spectrum overlaps the acceptors' absorption spectrum (Feng et al., 2016; Wang et al., 2017a; Wu et al., 2011). Considering all the advantages mentioned above, MOF composites could serve as an ideal ECL donor. Using polydopamine (PDA) as effective quenchers and Cu^{2+} as inhibitors to the ECL emission of luminophore through energy transfer (Yue et al., 2015; Zhao et al., 2016), Ju's group fabricated a sensitive ECL immunosensor for procalcitonin determination based on Fe_3O_4@PDA-Cu_xO as double quenchers towards self-enhanced $Ru(bpy)_3^{2+}$ modified MOFs (Wang et al., 2019b). In another work, they reported a dual-quenching ECL-RET platform from Ru–In_2S_3 to α-MoO_3-Au for procalcitonin measurement (Xue et al., 2019a).

As for acceptor, various nanomaterials, including MOF composites, have been employed to design donor-acceptor pairs for ECL-RET applications (Wang et al., 2016a, 2016d). Due to their broad absorption spectra, tunable and stable optical property, large surface area, excellent biocompatibility, and ease of labelling, metallic nanomaterials, typical acceptors in the RET system (Jin and Gao, 2009; Wu et al., 2014), are widely employed as desirable quenchers in ECL-RET based sensing. In particular, Au NPs play a significant role in ECL-RET systems owing to a high extinction coefficient and a broad absorption spectrum (He et al., 2013). Due to the superior quenching effects of metal nanoparticles mentioned above, Wu's group synthesized two different ECL-active MOF composites with QDs as guests, both of which exhibited excellent ECL properties and were used separately as emitters for multiplexed detection of metal ions (Hg^{2+} and Pb^{2+}) and antibiotics (kanamycin and neomycin) (Feng et al., 2019, 2020). Upon adding the target, Au nanoparticles or Pt nanoparticles acted as signal quenchers due to ECL-RET between QDs and AuNPs (or Pt NPs). In another work, Zhao et al. prepared a sensitive ECL immunosensor for insulin measurement through ECL-RET between $Ru(bpy)_3^{2+}$ loaded inside the UiO-67 (donor) and Au NPs decorated on silicon spheres (acceptor) (Dong et al., 2016).

MOF composites can also serve as ECL-RET acceptors. For example, Fang et al. reported that the intensity and range of UV–visible absorption of NH_2-MIL-53 could be increased by the wide range of UV absorption of Pd NPs, thus synergistically quench the ECL signal of Au NPs-modified g-C_3N_4 nanosheets (g-C_3N_4@Au NPs) (Fang et al., 2019a). On the basis of spectral overlap between absorption spectrum of $Ru(bpy)_3^{2+}$ and ECL spectrum of g-C_3N_4 nanosheets, Wang et al. proposed a ratiometric ECL-RET aptasensor for sensitive Aβ protein determination based on the ECL-RET between g-C_3N_4 nanosheets and Ru@MOF (Wang et al., 2019f). Interestingly, the bare MOFs, such as Fe-MIL-88 MOFs (Fu et al., 2017), and MIL-125 (Dong et al., 2019), were also used as acceptors in ECL biosensing.

A comparison of different ECL-RET biosensors and sensors based on MOF composites is listed in Table 2. Despite ECL-RET-based strategies for all, they vary with each in detection limit. Generally, the sensitivity of RET-based sensors relies on not only the ECL intensity of the donor, but also the strategies coupled with other amplification methods and detection states (e.g., "signal-on'' or "signal-off'). Additionally, reaction conditions, especially the stability of MOF composites, are crucial factors that affect the detection limit. For instance, leakage of luminophores would result in high background, and some assisted approaches or innovative strategies should be included to enhance the sensing sensitivity.

4. Applications of MOF-based ECL systems

ECL-active MOFs have been widely applied in biosensors due to their distinct characteristics in selective capture of analytes (Hu et al., 2014; Liao et al., 2019). Here, recent advances in MOF-based analysis are described with a focus on immunoassay, ECL genosensors, and small molecule detection.

4.1. ECL immunoassay

ECL immunoassay has gained much interest in biomedical applications due to the integration of the specific immunoreactions with the intrinsic properties of ECL. Cancers have long been the major health threat worldwide, and the cancer markers, such as NT-proBNP, Aβ, CEA, and PSA, associated with certain tumors play important roles in diseases diagnosis, implying the necessity to develop ultrasensitive detection methods for early and sensitive determination of disease markers. For instance, increased concentration of NT-proBNP is considered as a biomarker for diagnosis of heart failure (Richards and Troughton, 2004). Biocompatible Ce-MOF@g-C_3N_4/Au nanocomposites were used as signal-amplified ECL probes for label-free NT-proBNP immunoassay (Li et al., 2019). The porous matrix of Ce-MOF not only amplified the ECL signal of g-C_3N_4 nanosheets, but also obviously improved their interfacial stability. In another work, Xiong et al. designed a signal amplified ECL sensor for sensitive NT-proBNP measurement by employing $[Ru(dcbpy)_3]^{2+}$ doped MOFs as ECL nano-labels due to the excellent accumulation capability of MOFs towards $[Ru(dcbpy)_3]^{2+}$

Table 2
A brief summary of the ECL-RET biosensors and sensors based on ECL-active MOF composites.

Analyte	Donor	Emission wavelength (nm)	Acceptor	Absorption wavelength (nm)	LOD	Reference
Aβ	g-C_3N_4@Au NPs		Pd NPs@NH_2-MIL-53		3.4 fg/mL	Fang et al. (2019a)
Aβ	Ru(bpy)$_3^{2+}$/zinc oxalate MOFs		Au@NiFe MOFs	550	13.8 fg/mL	Zhao et al. (2019)
Aβ	g-C_3N_4 nanosheet	460	Ru@MOF	450, 520	3.9 fg/mL	Wang et al. (2019f)
dopamine	3,4,9,10-perylenetetracar-boxylic acid (PTCA)	425–600	Fe-MIL-88 MOFs	500–700	0.29 pM	Fu et al. (2017)
Hg^{2+}; Pb^{2+}	MIL-53(Al)@CdTe		AuNPs/PtNPs	525/270	4.1 pM; 37 pM	Feng et al. (2020)
Insulin	UiO-67/Ru(bpy)$_3^{2+}$		Au@SiO_2		1 pg/mL	Zhao et al. (2018)
Insulin	Pb-β-CD	400–600	CRuSi NPs	400–500	0.042 pg/mL	Ma et al. (2016a)
Kanamycin; neomycin	MIL-53(Fe)@CdS	517	AuNPs	515	0.017 pM; 0.35 nM	Feng et al. (2019)
NT-proBNP	AgNC-sem@AuNPs	740	MIL-125	406–900	0.11 pg/mL	Dong et al. (2019)
procalcitonin	Ru@MIL-101	630	Fe_3O_4@PDA-Cu_xO		0.18 pg/mL	Wang et al. (2019b)
procalcitonin	Ru–In_2S_3		α-MoO_3-Au		12.49 fg/mL	Xue et al. (2019a)

(Xiong et al., 2015). Aβ has been recognized as one of the reliable indicators for diagnosis of Alzheimer's disease, implicating the importance of sensitive detection of Aβ for early assessment of Alzheimer's disease. Cao's group fabricated a sensitive immunosensor for Aβ determination by using NH_2-UiO-66 and MIL-101, which can increase the immobilization amount of antibodies due to excellent porosity and abundant functional groups within these dual MOFs (Dong et al., 2020). In another report, an ultrasensitive immunosensor was fabricated for Aβ determination *via* ECL-RET between Au nanoparticles-loaded g-C_3N_4 nanosheets and Pd NPs coated NH_2-MIL-53 for signal amplification (Fang et al., 2019a). Au NPs not only enhanced the ECL signal of g-C_3N_4, but also increased the biocompatibility of g-C_3N_4 for antibody modification. A notable diminishing ECL signal can be observed when incubating Pd NPs@NH_2-MIL-53 onto the immunosensor because Pd NPs@NH_2-MIL-53(Al) can quench the ECL signal of g-C_3N_4@Au NPs (Fig. 6), enabling ultrasensitive and selective determination of Aβ.

Since its first report by Yuan's group in 2014 (Zhuo et al., 2014), the signal amplification strategy of self-enhanced ECL complex has been successfully applied in ECL immunosensors. For example, an intramolecular self-enhanced ECL immunosensor was proposed for procalcitonin quantification due to the existence of Ru(bpy)$_3^{2+}$ and its co-reactant (PEI) in the same complex (Wang et al., 2019b). More importantly, the leakage of Ru(bpy)$_3^{2+}$ was hampered tactfully because of PEI decorated on the surface of Ru(bpy)$_3^{2+}$ doped MOFs. The Ru(bpy)$_3^{2+}$-PEI enriched MIL-101(Al)–NH_2 MOF with high emission efficiency was used to establish a "signal off" ECL immunosensing platform. In another report, on the basis of proximity-induced intramolecular DNA strand displacement, PCN-777 was used as an excellent nanocarrier of Ru(bpy)$_2$(mcpbpy)$^{2+}$ luminophore and co-reactant PEI to synthesize self-enhanced ECL complex for MUC1 immunosensing (Hu et al., 2018).

All the above self-enhanced ECL immunosensors achieved successful target detection. A summary of different MOF composites for ECL

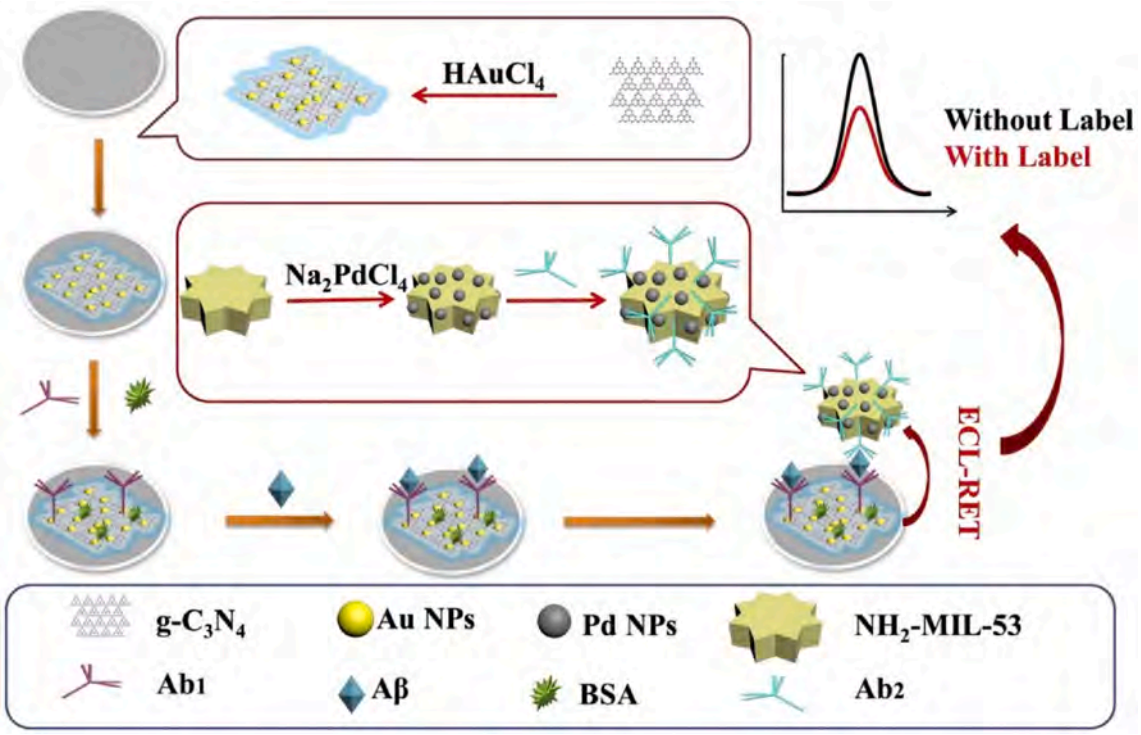

Fig. 6. (A) Schematic illustration of the ECL immunosensor (reproduced from (Fang et al., 2019a) with permission from Elsevier).

immunoassay is listed in Table 3.

4.2. ECL genosensors

Of late, a series of powerful signal amplification techniques, such as rolling circle amplification (RCA) (Wang et al., 2019d; Zheng et al., 2018b), hybridization chain reaction (HCR) (Qing et al., 2019; Lu et al., 2017), and catalytic hairpin assembly (CHA) (Qing et al., 2020; Zhou et al., 2020a), have been widely used in genosensors. The past 5 years has witnessed great development of MOF-based ECL genosensors coupled with various amplification strategies, and a variety of sensing platforms have been proposed to enhance their sensitivity and selectivity.

MicroRNAs (miRNAs), an emerging series of small (19–23 nt) non-coding RNAs, have become reliable biomarkers for cancers and various genetic disorders (Peng et al., 2017; Ye et al., 2016). Therefore, it is important to develop ultrasensitive, reliable and universal detection platforms for miRNAs detection. To date, several MOF-based ECL biosensors have been reported for accurate analysis of miRNAs. Based on ruthenium-functionalized 2D MOF nanosheets as the signal unit, Guo's group developed an efficient Faraday-cage ECL biosensor for miRNA-141 determination by immobilizing the capture DNA on the functionalized magnetic nanospheres as the capture unit (Shao et al., 2018b). Moreover, inspired by the strong ECL emissions at different potentials of g-C_3N_4@AuNPs and Ru-MOF, they proposed a potential-resolved Faraday cage-type ECL system for simultaneous detection of miRNAs using two signal units of g-C_3N_4@AuNPs-sDNA1 and Ru-MOF-sDNA2 (Shao et al., 2018a). In the absence of miRNA-141 and miRNA-21, the two ECL signal units were away from the electrode, implying weak ECL signals. Upon addition of miRNAs, DNA hybridization can be triggered on the electrode surface. The separate accumulation of g-C_3N_4 and MOF nanosheet probes on the electrodes can be directly analyzed, achieving the simultaneous quantification of two miRNAs (Fig. 7). In another work, Jian et al. reported an ion-responsive ECL genosensor for determination of miRNA-155 by combining strand displacement reaction with $Ru(bpy)_3^{2+}$-functionalized MOFs that could be disassembled in the presence of Hg^{2+} and release large quantities of $Ru(bpy)_3^{2+}$, thus producing a strong ECL signal (Jian et al., 2018). Through rational design of DNA sequences, these methods can be employed to measure a broad range of nucleic acids, which facilitates the construction of controllable disassembly of DNA devices for diverse applications.

In recent years, many functional oligonucleotides, such as aptamers and DNAzymes, have been selected *in vitro*. Aptamers are single nucleic acid chains with specific interaction with targets (Liu et al., 2014a; Zhou and Rossi, 2017). Thus, aptamers can be used to fabricate aptasensors with the advantages of easy synthesis and modification, high reliability, low cost, easy storage. Owing to their unique properties, ECL active MOF-based aptasensors have been constructed for determination of a wide range of targets. For instance, a self-enhanced ECL aptasensor based on 2D MOF layers as ECL signal amplification labels and ferrocene as the quenching elements achieved the ultrasensitive detection of MUC1 (Yang et al., 2019). In another work, a dual gears ECL aptasensor for multiplexed quantification of kanamycin and neomycin was fabricated with MIL-53(Fe) as carriers of CdS QDs and Au NPs (or Pt NPs) as quenchers (Feng et al., 2019). Aside from proteins and small molecules, ECL aptasensors have also been utilized for detection of metal ions. Feng et al. designed a sensitive ECL aptasensor for multiple determination of Hg^{2+} and Pb^{2+} by using MIL-53(Al)@CdTe-PEI and AuNPs (or PtNPs) labelled aptamer as ECL signal probe and target recognition probe, respectively (Feng et al., 2020). The aptasensor realized the determination of Hg^{2+} and Pb^{2+} in fish and shrimp samples with good recoveries.

DNAzyme as the specific sensing unit has been used for signal amplification in ECL genosensors (Wang et al., 2018a; Zhang et al., 2015b). For example, Shao et al. proposed a specific ratiometric ECL platform for PSA detection by using DNAzyme modified MOFs as both quenchers and enhancers with QDs and luminol as ECL emitters (Shao et al., 2018c). Complementary DNA modified near-infrared QDs were immobilized onto the surface of GCE to trigger the sequential hybridization among different probes. Upon adding PSA, the DNAzyme modified probes would stay away from the electrode surface because of the specific binding between aptamer and PSA, switching the ECL signals (QDs-luminol) from "off-on" state to "on-off" state. This novel biosensor achieved not only signal self-calibration but also synergistic amplification.

Table 3
Electroactive MOF composites strategies for immunoassay.

Target	MOF composites	Linear range	LOD	Relative standard deviations (%)	Reference
Aβ	Pd NPs@NH_2-MIL-53	10 fg/mL to 50 ng/mL	3.4 fg/mL	2.2–3.6	Fang et al. (2019a)
Aβ	zinc oxalate MOFs	100 fg/mL to 50 ng/mL	13.8 fg/mL	0.41–3.7	Zhao et al. (2019)
Aβ	Co-MOFs/ABEI	10 fg/mL to 100 ng/mL	3 fg/mL	2.64	Wang et al. (2019a)
Aβ	$Ru(bpy)_3^{2+}$@NH_2-UiO-66	10^{-5} ng/mL to 50 ng/mL	3.32 fg/mL	0.44–3.01	Dong et al. (2020)
CA 15-3	$Ru(bpy)_3^{2+}$@UiO-66-NH_2	5×10^{-4} to 5×10^{2} U/mL	1.7705×10^{-5} U/mL	1.87–2.31	Xiong et al. (2019)
cardiac troponin I	2D Ru-MOF nanosheets	1 fg/mL to 10 ng/mL	0.48 fg/mL	1.44–3.11	Yan et al. (2019)
CEA	MIL-101-CdSe	10^{-12} to 10^{-4} mg/mL	0.33 fg/mL	1.75	Liu et al. (2017)
CEA	Ru/Cu/Ni MOFs	0.1 pg/mL to 100 ng/mL	0.027 pg/mL	0.20–1.4	Li et al. (2017b)
CEA	AuNP@NPCGO	0.01–80 ng/mL	3 pg/mL	2.84–5.57	Huang et al. (2018)
cTnI	luminol-AgNPs@ZIF-67	1 fg/mL to 1 μg/mL	0.58 fg/mL	5	Wang et al. (2019e)
cTnI	CdTe@IRMOF-3@CdTe	1.1 fg/mL to 11 ng/mL	0.46 fg/mL	0.92	Yang et al. (2018)
DES	$Ru(bpy)_3^{2+}$/UiO-67	0.01 pg/mL to 50 ng/mL	3.27 fg/mL	2.7	Dong et al. (2018)
h-FABP	Ru-MOF	150 fg/mL to 150 ng/mL	2.6 fg/mL	1.57–3.42	Qin et al. (2018)
human copeptin	GO-TEOA@MOFs	5 pg/mL to 500 ng/mL	360 fg/mL	1.5	Qin et al. (2019)
Insulin	Pb-β-CD	0.1 pg/mL to 10.0 ng/mL	0.042 pg/mL	5	Ma et al. (2016a)
Insulin	UiO-67/$Ru(bpy)_3^{2+}$	0.0025–50 ng/mL	1 pg/mL		Zhao et al. (2018)
mucin1	ABEI@Fe-MIL-101	1 fg/mL to 1 ng/mL	0.26 fg/mL	3.05	Jiang et al. (2017)
mucin1	Ru–PCN-777	100 fg/mL to 100 ng/mL	33.3 fg/mL	1.2–4.7	Hu et al. (2018)
mucin1	ABEI/MIL-101(Fe)	10 fg/mL to 10 ng/mL	1.6 fg/mL	4.42	Wang et al. (2018b)
mucin 1	PEI@Ru-Hf-MOL	1 fg/mL to 10 ng/mL	0.48 fg/mL	2.1–7.4	Hu et al. (2019)
NT-proBNP	MOFs	5 pg/mL to 25 ng/mL	1.67 pg/mL		Xiong et al. (2015)
NT-proBNP	Ce-MOF@g-C_3N_4	0.005–20 ng/mL	3.59 pg/mL	1.3	Li et al. (2019)
PSA	MIL-53(Fe)–NH_2	1 pg/mL to 300 ng/mL	0.2 pg/mL		Khoshfetrat et al. (2019)
PSA	Ag@Pb(II)-β-CD	0.001–50 ng/mL	0.34 pg/mL	0.17–0.84	Ma et al. (2016b)
Procalcitonin	Ru@MIL-101	0.5 pg/mL to 100 ng/mL	0.18 pg/mL		Wang et al. (2019b)
kexin type 9	Ce-TCPP-MOF	50 fg/mL to 10 ng/mL	19.12 ± 2.69 fg/mL	5.26–6.37	Zhou et al., 2020b

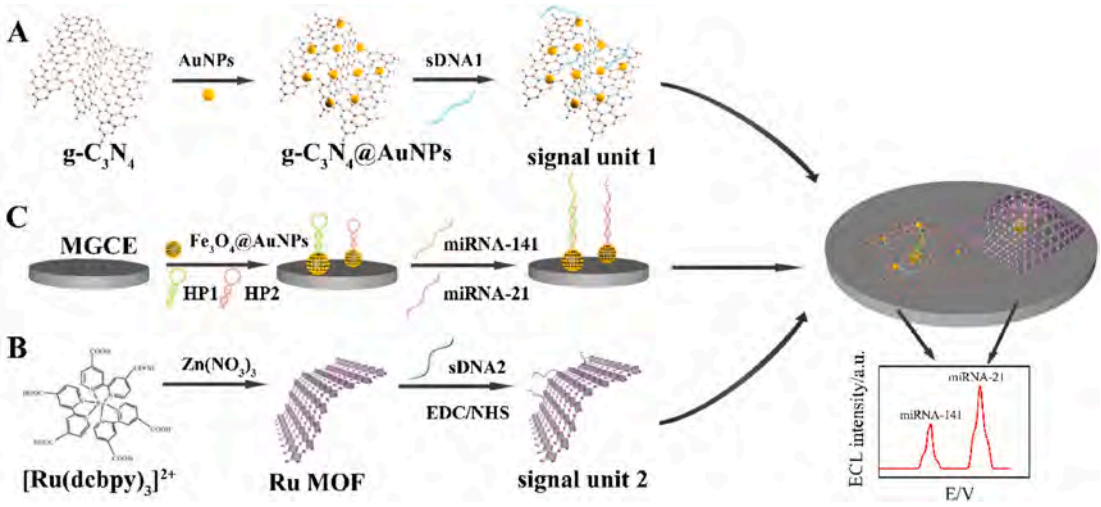

Fig. 7. Schematic Illustration of (A) signal unit 1 (g-C_3N_4@AuNPs-sDNA1), (B) signal unit 2 (Ru-MOF-sDNA2), and (C) the proposed potential-resolved Faraday cage-type ECL biosensor for simultaneous determination of miRNA-141 and miRNA-21. (reproduced from (Shao et al., 2018a) with permission from Elsevier).

4.3. Small molecules

For small molecule quantification, most strategies depend on the specific recognition between aptamers and target molecules. Based on this mechanism, a wide range of molecules have been sensitively and selectively measured based on MOFs. Using the inhibition effect of small molecules on ECL intensity, dopamine and deoxynivalenol have also been detected by MOF-based solid-state ECL (Cai et al., 2018; Li et al., 2018), and MOF-integrated co-reaction accelerator system (Zheng et al., 2018a), respectively.

Metal ions have also been detected due to the serious side effects of either their deficiency or overdose on human health and environment (Aragay et al., 2011). Currently, there is an ongoing research on sensing strategies for trace heavy metal detection. Standard methods for analyzing metal ions mainly include inductively coupled plasma mass spectrometry (ICP-MS) (Caroli et al., 1999), atomic absorption spectroscopy (AAS) (Pohl, 2009), and mass spectroscopy (MS) (Flamini and Panighel, 2006). However, these methods usually require expensive instruments and specialized personnel for operation. Recently, MOF-based sensors have been proposed for metal ions quantification. For example, by immobilizing $Ru(bpy)_3^{2+}$-UiO66 MOF on NH_2–SiO_2 modified GCE electrode *via* forming amide bonds, a sensor was constructed for Pb^{2+} quantification because of the high quenching capability of Pb^{2+} to the ECL intensity of the $Ru(bpy)_3^{2+}$ (Shan et al., 2019). Similarly, a novel copper (II) MOF (Cu-MOF) was successfully prepared by facile one step hydrothermal method and then applied to fabricate a sensor for Fe^{2+} measurement (Tang et al., 2019). The inhibition effect of Fe^{2+} on ECL signal enabled ultrasensitive quantification of Fe^{2+} with a detection limit down to 40 pM in environmental water samples.

5. Conclusions

Recent years have witnessed the development of MOF-based ECL sensing with representative examples. On the basis of unique properties of high guest molecule loading, controllable composition and structure, versatile functionality, and improved biocompatibility, MOFs have been shown as promising candidates in ECL applications, and various MOF composites have been designed for novel ECL applications, varying from individual MOF to multifunctional MOF composites. In this review, we have summarized three different strategies to design ECL-active MOF composites including using luminophore as a ligand, *in situ* encapsulation of luminophore within the framework, and post-synthetic modification. The excellent properties of MOF composites have drawn much attention as innovative emitters, supporters of ECL luminophores, electrode modification materials and co-reaction accelerators in ECL systems, owing to their high load ability, large surface area, and excellent catalytic activity. In addition, MOF composites can be used not only as emitters but also donors or acceptors in ECL-RET strategies. With the newly emerged excellent properties MOF composites and coreactants, coupled with various signal amplification strategies, MOF composites have been successfully applied in immunoassays, genosensors, aptasensors, and small molecule detection. Furthermore, due to the rapid development of MOFs in biosensing, bioimaging, and biomedicine, the efficiency of ECL biosensing strategies can be improved by using various novel MOFs, such as new ECL emitters with excellent properties and high efficiencies, multifunctional MOF composites, etc.

By integrating functional materials into MOFs, MOF composites exhibited the following advantages: (1) Conjugation with proteins (antibody, enzyme) endows MOF composites with high accessibility to the recognition sites from all sides, enabling the ECL signal to be amplified in a constrained area. (2) MOFs' high porosity and tunable structures facilitate the diffusion of the substrate easily, which greatly enhances the reaction efficiency. (3) The high surface area of MOFs is a good platform to load more other functional materials, which is beneficial to design novel ECL biosensors. (4) Using all-in-one MOF composites achieves the synergic effects and novel potentialities among individual parts for signal transduction in ECL biosensors. Therefore, the recent development of MOF composites based ECL sensing may fuel further growth of the ECL technology.

6. Future outlooks

Actually, the researches of ECL-active MOF composites are still at an infant stage and are facing tough challenges. To further promote its biosensing application and improve its analytical performance, the following aspects should be considered in future work: (1) Incorporate functional moieties, including luminophore and active nanoparticles, in MOFs with multiple functions. Thus, MOFs will become promising candidates for ECL applications due to multi-functionality within multi-component MOFs. (2) Achieve sensitive measurement of analytes by combining MOF-based ECL sensing with multifarious signal amplification strategies. To improve detection sensitivity, various enzyme-assiated methods have been introduced with detection limits at the subattomole levels, which are comparable to or even better than the levels attainable by PCR. Enzyme-assisted methods, despite ultrahigh sensitivity, are involved in harsh reaction conditions and complex procedures, and using enzymes in MOF-based ECL is incompatible with simple, fast and convenient analysis requirements. Therefore, new MOF-

based ECL biosensing strategies should be integrated with novel efficient sensing methodologies. (3) Find more suitable MOFs as donors or acceptors for ECL-RET by controlling the distance and the desirable linkages between donors and acceptors. (4) Select highly efficient aptamers. The development of aptamers benefits the adaptation of MOF-based ECL systems, which have been employed to quantify a great variety of analytes. However, there is still a gap to develop aptamer-MOF ECL biosensors due to the limited number of aptamers. (5) Carry out practical applications. The current MOF-based ECL systems are in the laboratory stage, and their commercial applications remains a substantial challenge. Future research in MOFs may pave way for practical applications, such as exploring portable devices and field instruments for environmental applications. Therefore, development of novel luminophores and co-reactors with high stability, nontoxicity or low-toxicity, good biocompatibility, and high ECL efficiency is highly essential to that purpose. The marriage of MOF and ECL principles will facilitate the development of new devices with high performance and practical applications.

Declaration of competing interest

The authors declare that they have no known competing financial interests or personal relationships that could have appeared to influence the work reported in this paper.

Acknowledgements

We gratefully appreciate the support from National Natural Science Foundation of China (21778020, 21804046) and Sci-tech Innovation Foundation of Huazhong Agriculture University (2662017PY042). We thank Zhen Wang for help with the TOC figure drawing.

References

Aguilera-Sigalat, J., Bradshaw, D., 2016. Coord. Chem. Rev. 307, 267–291.
Ai, L., Li, L., Zhang, C., Fu, J., Jiang, J., 2013. Chem. Eur J. 19, 15105–15108.
Aragay, G., Pons, J., Merkoçi, A., 2011. Chem. Rev. 111, 3433–3458.
Cai, M., Loague, Q.R., Zhu, J., Lin, S., Usov, P.M., Morris, A.J., 2018. Dalton Trans. 47, 16807–16812.
Cao, J.T., Liu, F.R., Fu, X.L., Ma, J.X., Ren, S.W., Liu, Y.M., 2019. Chem. Commun. 55, 2829–2832.
Cao, Y., Yuan, R., Chai, Y., Mao, L., Niu, H., Liu, H., Zhuo, Y., 2012. Biosens. Bioelectron. 31, 305–309.
Caroli, S., Forte, G., Iamiceli, A.L., Galoppi, B., 1999. Talanta 50, pp. 327–336.
Carrara, S., Arcudi, F., Prato, M., De Cola, L., 2017. Angew. Chem. Int. Ed. 56, 4757–4761.
Chen, D., Li, B., Jiang, L., Duan, D., Li, Y., Wang, J., He, J., Zeng, Y., 2015. RSC Adv. 5, 97910–97917.
Chen, M.M., Wang, Y., Cheng, S.B., Wen, W., Zhang, X., Wang, S., Huang, W.H., 2018. Anal. Chem. 90, 5075–5081.
Cunha, D., Ben Yahia, M., Hall, S., Miller, S.R., Chevreau, H., Elkaïm, E., Maurin, G., Horcajada, P., Serre, C., 2013. Chem. Mater. 25, 2767–2776.
Della Rocca, J., Liu, D., Lin, W., 2011. Accounts Chem. Res. 44, 957–968.
Deng, S., Zhang, T., Ji, X., Wan, Y., Xin, P., Shan, D., Zhang, X., 2015. Anal. Chem. 87, 9155–9162.
Ding, Z., Quinn, B.M., Haram, S.K., Pell, L.E., Korgel, B.A., Bard, A.J., 2002. Science 296, 1293–1297.
Dong, X., Zhao, G., Li, X., Fang, J., Miao, J., Wei, Q., Cao, W., 2020. Talanta 208, 120376.
Dong, X., Zhao, G., Li, X., Miao, J., Fang, J., Wei, Q., Cao, W., 2019. Mikrochim. Acta 186, 811.
Dong, X., Zhao, G., Liu, L., Li, X., Wei, Q., Cao, W., 2018. Biosens. Bioelectron. 110, 201–206.
Dong, Y.P., Zhou, Y., Wang, J., Zhu, J.J., 2016. Anal. Chem. 88, 5469–5475.
Dou, S., Dong, C.-L., Hu, Z., Huang, Y.-C., Chen, J.-l., Tao, L., Yan, D., Chen, D., Shen, S., Chou, S., Wang, S., 2017. Adv. Funct. Mater. 27, 1702546.
Fang, J., Zhao, G., Dong, X., Li, X., Miao, J., Wei, Q., Cao, W., 2019a. Biosens. Bioelectron. 142, 111517.
Fang, Q., Lin, Z., Lu, F., Chen, Y., Huang, X., Gao, W., 2019b. Electrochim. Acta 302, 207–215.
Feng, D., Li, P., Tan, X., Wu, Y., Wei, F., Du, F., Ai, C., Luo, Y., Chen, Q., Han, H., 2020. Anal. Chim. Acta 1100, 232–239.
Feng, D., Tan, X., Wu, Y., Ai, C., Luo, Y., Chen, Q., Han, H., 2019. Biosens. Bioelectron. 129, 100–106.
Feng, D., Wu, Y., Tan, X., Chen, Q., Yan, J., Liu, M., Ai, C., Luo, Y., Du, F., Liu, S., Han, H., 2018. Sensor. Actuator. B Chem. 265, 378–386.
Feng, Q.M., Shen, Y.Z., Li, M.X., Zhang, Z.L., Zhao, W., Xu, J.J., Chen, H.Y., 2016. Anal. Chem. 88, 937–944.
Flamini, R., Panighel, A., 2006. Mass Spectrom. Rev. 25, 741–774.
Fu, X., Yang, Y., Wang, N., Chen, S., 2017. Sensor. Actuator. B Chem. 250, 584–590.
Gülbağça, F., Arıkan, K., Cellat, K., Khan, A., Şen, F., 2019. Metal organic frameworks (MOF's) for biosensing and bioimaging applications. In: Khan, A., Verpoort, F., Rahman, M.M., Isa, I.M., Asiri, A.M., Rub, M.A. (Eds.), Metal-Organic Framework Composites. Volume II. Materials Research Forum, USA, pp. 308–360.
Gao, W.Y., Chrzanowski, M., Ma, S., 2014. Chem. Soc. Rev. 43, 5841–5866.
Ge, L., Wang, L., Rudolph, V., Zhu, Z., 2013. RSC Adv. 3, 25360–25366.
Han, Z., Yang, Z., Sun, H., Xu, Y., Ma, X., Shan, D., Chen, J., Huo, S., Zhang, Z., Du, P., Lu, X., 2019. Angew. Chem. Int. Ed. 58, 5915–5919.
He, L.J., Wu, M.S., Xu, J.J., Chen, H.Y., 2013. Chem. Commun. 49, 1539–1541.
Hercules, D.M., 1964. Science 145, 808–809.
Hu, G.B., Xiong, C.Y., Liang, W.B., Yang, Y., Yao, L.Y., Huang, W., Luo, W., Yuan, R., Xiao, D.R., 2019. Biosens. Bioelectron. 135, 95–101.
Hu, G.-B., Xiong, C.-Y., Liang, W.-B., Zeng, X.-S., Xu, H.-L., Yang, Y., Yao, L.-Y., Yuan, R., Xiao, D.-R., 2018. ACS Appl. Mater. Interfaces 10, 15913–15919.
Hu, Z., Deibert, B.J., Li, J., 2014. Chem. Soc. Rev. 43, 5815–5840.
Huang, W., Hu, G.B., Yao, L.Y., Yang, Y., Liang, W.B., Yuan, R., Xiao, D.R., 2020. Anal. Chem. 92, 3380–3387.
Huang, X., Deng, X., Qi, W., Wu, D., 2018. New J. Chem. 42, 13558–13564.
Huang, Y., Zhao, M., Han, S., Lai, Z., Yang, J., Tan, C., Ma, Q., Lu, Q., Chen, J., Zhang, X., Zhang, Z., Li, B., Chen, B., Zong, Y., Zhang, H., 2017. Adv. Mater. 29.
Huxford, R.C., Della Rocca, J., Lin, W., 2010. Curr. Opin. Chem. Biol. 14, 262–268.
Irkham, Watanabe, T., Fiorani, A., Valenti, G., Paolucci, F., Einaga, Y., 2016. J. Am. Chem. Soc. 138, 15636–15641.
Jian, Y., Wang, H., Lan, F., Liang, L., Ren, N., Liu, H., Ge, S., Yu, J., 2018. Mikrochim. Acta 185, 133.
Jiang, X., Chai, Y., Yuan, R., Cao, Y., Chen, Y., Wang, H., Gan, X., 2013. Anal. Chim. Acta 783, 49–55.
Jiang, X., Wang, H., Yuan, R., Chai, Y., 2015. Biosens. Bioelectron. 63, 33–38.
Jiang, X., Wang, Z., Wang, H., Zhuo, Y., Yuan, R., Chai, Y., 2017. Chem. Commun. 53, 9705–9708.
Jin, Y., Gao, X., 2009. Nat. Nanotechnol. 4, 571–576.
Karimi, Z., Morsali, A., 2013. J. Mater. Chem. 1, 3047.
Kent, C.A., Mehl, B.P., Ma, L., Papanikolas, J.M., Meyer, T.J., Lin, W., 2010. J. Am. Chem. Soc. 132, 12767–12769.
Khoshfetrat, S.M., Khoshsafar, H., Afkhami, A., Mehrgardi, M.A., Bagheri, H., 2019. Anal. Chem. 91, 6383–6390.
Kozachuk, O., Luz, I., Llabrés i Xamena, F.X., Noei, H., Kauer, M., Albada, H.B., Bloch, E. D., Marler, B., Wang, Y., Muhler, M., Fischer, R.A., 2014. Angew. Chem. Int. Ed. 53, 7058–7062.
Lee, J., Farha, O.K., Roberts, J., Scheidt, K.A., Nguyen, S.T., Hupp, J.T., 2009. Chem. Soc. Rev. 38, 1450–1459.
Lei, J., Qian, R., Ling, P., Cui, L., Ju, H., 2014. TrAC Trends Anal. Chem. (Reference Ed.) 58, 71–78.
Li, G., Yu, X., Liu, D., Liu, X., Li, F., Cui, H., 2015. Anal. Chem. 87, 10976–10981.
Li, L., Zhao, Y., Li, X., Ma, H., Wei, Q., 2019. J. Electroanal. Chem. 847, 113222.
Li, S.K., Chen, A.Y., Niu, X.X., Liu, Z.T., Du, M., Chai, Y.Q., Yuan, R., Zhuo, Y., 2017a. Chem. Commun. 53, 9624–9627.
Li, X., Yu, S., Yan, T., Zhang, Y., Du, B., Wu, D., Wei, Q., 2017b. Biosens. Bioelectron. 89, 1020–1025.
Li, Y., Yang, L., Peng, Z., Huang, C., Li, Y., 2018. Anal. Methods 10, 1560–1564.
Liao, X., Fu, H., Yan, T., Lei, J., 2019. Biosens. Bioelectron. 146, 111743.
Lin, X., Luo, F., Zheng, L., Gao, G., Chi, Y., 2015. Anal. Chem. 87, 4864–4870.
Liu, Q., Jin, C., Wang, Y., Fang, X., Zhang, X., Chen, Z., Tan, W., 2014a. NPG Asia Mater. 6, 95.
Liu, Q., Yang, Y., Liu, X.-P., Wei, Y.-P., Mao, C.-J., Chen, J.-S., Niu, H.-L., Song, J.-M., Zhang, S.-Y., Jin, B.-K., Jiang, M., 2017. Sensor. Actuator. B Chem. 242, 1073–1078.
Liu, Y., Chen, X., Wang, M., Ma, Q., 2018. Green Chem. 20, 5520–5527.
Liu, Y., Zhang, W., Li, S., Cui, C., Wu, J., Chen, H., Huo, F., 2014b. Chem. Mater. 26, 1119–1125.
Liu, Y.L., Zhao, X.J., Yang, X.X., Li, Y.F., 2013. Analyst 138, 4526–4531.
Liu, Z., Qi, W., Xu, G., 2015. Chem. Soc. Rev. 44, 3117–3142.
Lu, S., Hu, T., Wang, S., Sun, J., Yang, X., 2017. ACS Appl. Mater. Interfaces 9, 167–175.
Ma, H., Li, X., Yan, T., Li, Y., Liu, H., Zhang, Y., Wu, D., Du, B., Wei, Q., 2016a. ACS Appl. Mater. Interfaces 8, 10121–10127.
Ma, H., Li, X., Yan, T., Li, Y., Zhang, Y., Wu, D., Wei, Q., Du, B., 2016b. Biosens. Bioelectron. 79, 379–385.
Ma, J., Wu, L., Li, Z., Lu, Z., Yin, W., Nie, A., Ding, F., Wang, B., Han, H., 2018. Anal. Chem. 90, 7415–7421.
Miao, W., 2008. Chem. Rev. 108, 2506–2553.
Miao, Y.R., Su, Z., Suslick, K.S., 2017. J. Am. Chem. Soc. 139, 4667–4670.
Mo, G., Qin, D., Jiang, X., Zheng, X., Mo, W., Deng, B., 2020. Sensor. Actuator. B Chem. 310, 127852.
Osman, D.I., El-Sheikh, S.M., Sheta, S.M., Ali, O.I., Salem, A.M., Shousha, W.G., El-Khamisy, S.F., Shawky, S.M., 2019. Biosens. Bioelectron. 141, 111451.
Peng, H., Huang, Z., Deng, H., Wu, W., Huang, K., Li, Z., Chen, W., Liu, J., 2019. Angew. Chem. Int. Ed. 58, 1–5.
Peng, L., Zhang, P., Chai, Y., Yuan, R., 2017. Anal. Chem. 89, 5036–5042.
Pohl, P., 2009. TrAC Trends Anal. Chem. (Reference Ed.) 28, 117–128.
Pu, G., Yang, Z., Wu, Y., Wang, Z., Deng, Y., Gao, Y., Zhang, Z., Lu, X., 2019. Anal. Chem. 91, 2319–2328.
Qi, X., Tian, H., Dang, X., Fan, Y., Zhang, Y., Zhao, H., 2019. Anal. Methods 11, 1111–1124.

Qin, X., Dong, Y., Wang, M., Zhu, Z., Li, M., Yang, D., Shao, Y., 2019. ACS Sens. 4, 2351–2357.
Qin, X., Zhang, X., Wang, M., Dong, Y., Liu, J., Zhu, Z., Li, M., Yang, D., Shao, Y., 2018. Anal. Chem. 90, 11622–11628.
Qing, Z., Hu, J., Xu, J., Zou, Zhen, Lei, Y., Qing, T., Yang, R., 2020. Chem. Sci. 11, 1985–1990.
Qing, Z., Xu, J., Hu, J., Zheng, J., He, L., Zou, Z., Yang, S., Tan, W., Yang, R., 2019. Angew. Chem. Int. Ed. 58, 2–14.
Raza, W., Kukkar, D., Saulat, H., Raza, N., Azam, M., Mehmood, A., Kim, K.-H., 2019. TrAC Trends Anal. Chem. (Reference Ed.) 120, 115654.
Ren, R., Cai, G., Yu, Z., Zeng, Y., Tang, D., 2018. Anal. Chem. 90, 11099–11105.
Richards, M., Troughton, R.W., 2004. Eur. J. Heart Fail. 6, 351–354.
Richter, M.M., 2004. Chem. Rev. 104, 3003–3036.
Santhanam, K.S.V., Bard, A.J., 1965. J. Am. Chem. Soc. 87, 139–140.
Shan, X., Pan, T., Pan, Y., Wang, W., Chen, X., Shan, X., Chen, Z., 2019. Electroanalysis 32, 462–469.
Shao, H., Lin, H., Lu, J., Hu, Y., Wang, S., Huang, Y., Guo, Z., 2018a. Biosens. Bioelectron. 118, 247–252.
Shao, H., Lu, J., Zhang, Q., Hu, Y., Wang, S., Guo, Z., 2018b. Sensor. Actuator. B Chem. 268, 39–46.
Shao, K., Wang, B., Nie, A., Ye, S., Ma, J., Li, Z., Lv, Z., Han, H., 2018c. Biosens. Bioelectron. 118, 160–166.
Shao, K., Wang, B., Ye, S., Zuo, Y., Wu, L., Li, Q., Lu, Z., Tan, X., Han, H., 2016. Anal. Chem. 88, 8179–8187.
Shao, K., Wang, J., Jiang, X., Shao, F., Li, T., Ye, S., Chen, L., Han, H., 2014. Anal. Chem. 86, 5749–5757.
Shu, J., Wang, W., Cui, H., 2015. Chem. Commun. 51, 11366–11369.
Stassen, I., Burtch, N., Talin, A., Falcaro, P., Allendorf, M., Ameloot, R., 2017. Chem. Soc. Rev. 46, 3185–3241.
Tang, T., Hao, Z., Yang, H., Nie, F., Zhang, W., 2019. J. Electroanal. Chem. 856, 113498.
Tokel, N.E., Keszthelyi, C.P., Bard, A.J., 1972. J. Am. Chem. Soc. 94, 4872–4877.
Vermoortele, F., Bueken, B., Le Bars, G., Van de Voorde, B., Vandichel, M., Houthoofd, K., Vimont, A., Daturi, M., Waroquier, M., Van Speybroeck, V., Kirschhock, C., De Vos, D.E., 2013. J. Am. Chem. Soc. 135, 11465–11468.
Wang, C., Liu, L., Liu, X., Chen, Y., Wang, X., Fan, D., Kuang, X., Sun, X., Wei, Q., Ju, H., 2020. Sensor. Actuator. B Chem. 307, 127619.
Wang, C., Zhang, N., Li, Y., Yang, L., Wei, D., Yan, T., Ju, H., Du, B., Wei, Q., 2019a. Sensor. Actuator. B Chem. 291, 319–328.
Wang, C., Zhang, N., Wei, D., Feng, R., Fan, D., Hu, L., Wei, Q., Ju, H., 2019b. Biosens. Bioelectron. 142, 111521.
Wang, H.-S., 2017. Coord. Chem. Rev. 349, 139–155.
Wang, H., Peng, L., Chai, Y., Yuan, R., 2017a. Anal. Chem. 89, 11076–11082.
Wang, J., Jiang, X., Han, H., 2016a. Biosens. Bioelectron. 82, 26–31.
Wang, J.X., Zhuo, Y., Zhou, Y., Wang, H.J., Yuan, R., Chai, Y.Q., 2016b. ACS Appl. Mater. Interfaces 8, 12968–12975.
Wang, L., Han, Y., Feng, X., Zhou, J., Qi, P., Wang, B., 2016c. Coord. Chem. Rev. 307, 361–381.
Wang, N., Wang, Z., Chen, L., Chen, W., Quan, Y., Cheng, Y., Ju, H., 2019c. Chem. Sci. 10, 6815–6820.
Wang, S., Lu, S., Zhao, J., Ye, J., Huang, J., Yang, X., 2019d. Biosens. Bioelectron. 126, 565–571.
Wang, S., Wang, Q., Shao, P., Han, Y., Gao, X., Ma, L., Yuan, S., Ma, X., Zhou, J., Feng, X., Wang, B., 2017b. J. Am. Chem. Soc. 139, 4258–4261.
Wang, S., Zhao, Y., Wang, M., Li, H., Saqib, M., Ge, C., Zhang, X., Jin, Y., 2019e. Anal. Chem. 91, 3048–3054.
Wang, Y., Shan, D., Wu, G., Wang, H., Ru, F., Zhang, X., Li, L., Qian, Y., Lu, X., 2018a. Biosens. Bioelectron. 106, 64–70.
Wang, Y., Zhang, Y., Sha, H., Xiong, X., Jia, N., 2019f. ACS Appl. Mater. Interfaces 11, 36299–36306.
Wang, Y.Z., Hao, N., Feng, Q.M., Shi, H.W., Xu, J.J., Chen, H.Y., 2016d. Biosens. Bioelectron. 77, 76–82.
Wang, Z., Jiang, X., Yuan, R., Chai, Y., 2018b. Biosens. Bioelectron. 121, 250–256.
Wei, H., Wang, E., 2008. TrAC Trends Anal. Chem. (Reference Ed.) 27, 447–459.
Wu, C.-D., Zhao, M., 2017. Adv. Mater. 29, 1605446.
Wu, M.S., He, L.J., Xu, J.J., Chen, H.Y., 2014. Anal. Chem. 86, 4559–4565.
Wu, M.S., Shi, H.W., Xu, J.J., Chen, H.Y., 2011. Chem. Commun. (J. Chem. Soc. Sect. D) 47, 7752–7754.
Wu, M.-X., Yang, Y.-W., 2017. Adv. Mater. 29, 1606134.
Xie, S., Dong, Y., Yuan, Y., Chai, Y., Yuan, R., 2016. Anal. Chem. 88, 5218–5224.
Xie, X., Wang, H., Zhang, L., Liu, Y., Chai, Y., Yuan, Y., Yuan, R., 2018. Sensor. Actuator. B Chem. 258, 1146–1151.
Xiong, C., Liang, W., Zheng, Y., Zhuo, Y., Chai, Y., Yuan, R., 2017. Anal. Chem. 89, 3222–3227.
Xiong, C.-Y., Wang, H.-J., Liang, W.-B., Yuan, Y.-L., Yuan, R., Chai, Y.-Q., 2015. Chem. Eur J. 21, 9825–9832.
Xiong, X., Zhang, Y., Wang, Y., Sha, H., Jia, N., 2019. Sensor. Actuator. B Chem. 297, 126812.
Xu, Y., Yin, X.-B., He, X.-W., Zhang, Y.-K., 2015. Biosens. Bioelectron. 68, 197–203.
Xue, J., Yang, L., Jia, Y., Zhang, Y., Wu, D., Ma, H., Hu, L., Wei, Q., Ju, H., 2019a. Biosens. Bioelectron. 142, 111524.
Xue, J., Yang, L., Wang, H., Yan, T., Fan, D., Feng, R., Du, B., Wei, Q., Ju, H., 2019b. Biosens. Bioelectron. 133, 192–198.
Yan, M., Ye, J., Zhu, Q., Zhu, L., Huang, J., Yang, X., 2019. Anal. Chem. 91, 10156–10163.
Yan, Z., Wang, F., Deng, P., Wang, Y., Cai, K., Chen, Y., Wang, Z., Liu, Y., 2018. Biosens. Bioelectron. 109, 132–138.
Yang, X., Yu, Y.-Q., Peng, L.-Z., Lei, Y.-M., Chai, Y.-Q., Yuan, R., Zhuo, Y., 2018. Anal. Chem. 90, 3995–4002.
Yang, Y., Hu, G.B., Liang, W.B., Yao, L.Y., Huang, W., Yuan, R., Xiao, D.R., 2019. Nanoscale 11, 10056–10063.
Yang, Y., Hu, G.B., Liang, W.B., Yao, L.Y., Huang, W., Zhang, Y.J., Zhang, J.L., Wang, J. M., Yuan, R., Xiao, D.R., 2020. Nanoscale 12, 5932–5941.
Yao, L.-Y., Yang, F., Liang, W.-B., Hu, G.-B., Yang, Y., Huang, W., Yuan, R., Xiao, D.-R., 2019. Sensor. Actuator. B Chem. 292, 105–110.
Ye, C., Wang, M.Q., Gao, Z.F., Zhang, Y., Lei, J.L., Luo, H.Q., Li, N.B., 2016. Anal. Chem. 88, 11444–11449.
Yue, X., Zhu, Z., Zhang, M., Ye, Z., 2015. Anal. Chem. 87, 1839–1845.
Zhang, G.-Y., Cai, C., Cosnier, S., Zeng, H.-B., Zhang, X.-J., Shan, D., 2016. Nanoscale 8, 11649–11657.
Zhang, H., Han, Z., Wang, X., Li, F., Cui, H., Yang, D., Bian, Z., 2015a. ACS Appl. Mater. Interfaces 7, 7599–7604.
Zhang, H., Li, M., Li, C., Guo, Z., Dong, H., Wu, P., Cai, C., 2015b. Biosens. Bioelectron. 74, 98–103.
Zhao, G., Wang, Y., Li, X., Dong, X., Wang, H., Du, B., Cao, W., Wei, Q., 2018. ACS Appl. Mater. Interfaces 10, 22932–22938.
Zhao, G., Wang, Y., Li, X., Yue, Q., Dong, X., Du, B., Cao, W., Wei, Q., 2019. Anal. Chem. 91, 1989–1996.
Zhao, M., Chen, A.Y., Huang, D., Zhuo, Y., Chai, Y.Q., Yuan, R., 2016. Anal. Chem. 88, 11527–11532.
Zhao, M., Wang, Y., Ma, Q., Huang, Y., Zhang, X., Ping, J., Zhang, Z., Lu, Q., Yu, Y., Xu, H., Zhao, Y., Zhang, H., 2015a. Adv. Mater. 27, 7372–7378.
Zhao, W.-W., Wang, J., Zhu, Y.-C., Xu, J.-J., Chen, H.-Y., 2015b. Anal. Chem. 87, 9520–9531.
Zheng, H., Yi, H., Dai, H., Fang, D., Hong, Z., Lin, D., Zheng, X., Lin, Y., 2018a. Sensor. Actuator. B Chem. 269, 27–35.
Zheng, J., Ji, X., Du, M., Tian, S., He, Z., 2018b. Nanoscale 10, 17206–17211.
Zhou, J., Rossi, J., 2017. Nat. Rev. Drug Discov. 16, 181–202.
Zhou, J., Wang, W., Li, S., Nie, A., Song, Z., Foda, M.F., Lu, Z., Zhao, L., Han, H., 2020a. Sensor. Actuator. B Chem. 304, 127267.
Zhou, Y., He, J., Zhang, C., Li, J., Fu, X., Mao, W., Li, W., Yu, C., 2020b. ACS Appl. Mater. Interfaces 12, 338–346.
Zhu, S., Lin, X., Ran, P., Xia, Q., Yang, C., Ma, J., Fu, Y., 2017. Biosens. Bioelectron. 91, 436–440.
Zhuo, Y., Liao, N., Chai, Y.-Q., Gui, G.-F., Zhao, M., Han, J., Xiang, Y., Yuan, R., 2014. Anal. Chem. 86, 1053–1060.